Coastal Marine Science 38(1): 27–41, 2015

Landsat image enhancement techniques for subtidal and intertidal seagrass detection and distribution mapping in the coastal waters of Sungai Pulai estuary, Malaysia

M. S. Hossain[1]*, B. Japar Sidik[2] and Z. Muta Harah[3,4]

*[1] *Department of Animal Science and Fishery, Faculty of Agriculture and Food Sciences, Universiti Putra Malaysia Bintulu Sarawak Campus, 97008 Bintulu, Sarawak, Malaysia.*
E-mail: shawkat@arannayk.org
[2] *Department of Biology, Faculty of Science, Universiti Putra Malaysia, 43400 UPM Serdang, Selangor Darul Ehsan, Malaysia.*
E-mail: japar@upm.edu.my
[3] *Department of Aquaculture, Faculty of Agriculture, Universiti Putra Malaysia, 43400 UPM Serdang, Malaysia.*
[4] *Institute of Bioscience, Universiti Putra Malaysia, 43400 UPM Serdang, Selangor Darul Ehsan, Malaysia.*
E-mail: muta@upm.edu.my
**Author for correspondence*

Received 23 June 2014; Accepted 28 October 2014

Abstract—In Malaysia, seagrasses commonly inhabit shallow intertidal waters, semi enclosed lagoons, mangroves, coral reef flats and shoals in subtidal zones. Seagrass meadows have widely been surveyed by field sampling methods. As an alternative means to field-based surveys, airborne and/or satellite based sensors have been used to produce cost-effective and, more importantly, repetitive sources of information on seagrass distribution over wider areas. The satellite-based sensors Landsat imagery have been used as relatively economic alternatives to aerial photographs to produce seagrass cover maps and change analysis. Two radiometric image enhancement techniques (ETs)—histogram equalization (HE) and manual enhancement (ME) were applied on the series of Landsat images for comparative analysis and assessing ability of ETs to recognize seagrass meadows within the subtidal and intertidal coastal waters of the Sungai Pulai estuary, Johor Straits, Malaysia. With a view to find relations between Mean Sea Level Tide Heights (MSLTHs) and results of ETs, actual 33 multi-date (1989–2014) images with a wide range of MSLTH regimes (−0.281 to 0.234 m) during image acquisition time, were processed by applying ETs. The ME substantially improved image quality compared to the HE, enabled detection of Seluyong seagrass meadows in intertidal mudflat, Merambong, Tanjung Adang Darat, Tanjung Adang Laut shoals in the subtidal areas. Seagrass meadows were 'easy-to-recognize' without noticeable variations due to MSLTH differences from the enhanced images acquired during extreme lowest spring tide height, −0.218 m and above until MSLTH at −0.085 m; found 'difficult-to-recognize' at full extent between −0.067 to −0.003 m and 'not-recognizable' above MSLTH. ETs would be ineffective if applied to images acquired higher than MSLTH (0.007 to 0.234 m). The proposed ET is found to provide a consistent and quantitative areal cover for seagrass mapping and understand past changes from multi-date image analyses.

Key words: Image enhancement technique, histogram equalization, manual enhancement, Landsat, seagrass, Malaysia

Introduction

Seagrass is widely distributed from tropical to subtropical coastal waters around the world. In Malaysia, seagrasses commonly inhabit shallow intertidal waters (Japar Sidik and Muta Harah 2003, Norhadi 1993), semi enclosed lagoon (Muta Harah et al. 2000), mangrove, coral reef flat (Japar Sidik et al. 2001) and shoal in subtidal zones (Japar Sidik et al. 2006); and are an important source of ecosystem goods and services for people dependent on coastal resources (Japar Sidik and Muta Harah 2011, Japar Sidik et al. 2006). The anthropogenic perturbations and natural causal agents have caused an average loss of 110 km^2 per year which is equivalent to 29% worldwide seagrass beds since the 19th century (GBO-3 2010). For the conservation and management of seagrass resources it is necessary to conduct periodic monitoring by field survey or applying remote sensing techniques (see review of Fortes, 2012 for remote sensing techniques).

Seagrass meadows have widely been surveyed by field sampling methods (Japar Sidik et al. 2006, Muta Harah and Japar Sidik 2013). As an alternative means to field-based surveys, airborne and/or satellite based sensors have been used to produce cost-effective and, more importantly, repetitive sources of information on seagrass distribution over wider

areas (Baumstark et al. 2013, Büttger et al. 2014). The satellite-based sensors Landsat imagery have been used as relatively economic alternatives to aerial photographs to produce seagrass cover maps and change analysis (Bouvet et al. 2003, Lyons et al. 2012). There are advantages and limitations of each technology due to spatial, spectral and temporal resolu-

Table 1. Advantage and limitations of remote sensing technologies and field-based data collection techniques for seagrass applications (Ferwerda et al. 2007, Xu and Zhao 2014, Brown et al. 2011, Malthus and Mumby 2003, Wang and Philpot 2007, Petus et al. 2014). Notes: TM=Thematic Mapper; ETM=Enhanced Thematic Mapper; SPOT=Satellite Pour l'Observation de la Terre; ALOS=Advanced Land Observing Satellite; ASTER=Advanced Spaceborne Thermal Emission and Reflection Radiometer; MODIS=Moderate-resolution Imaging Spectroradiometer; MERIS=MEdium Resolution Imaging Spectrometer; LiDAR=LIght Detection And Ranging; CASI=Compact Airborne Spectrographic Imager.

Platform	Sensor type (example)	Advantages	Constraints on application
Satellite	Hyperspectral (Hyperion)	High spectral (220 bands; 400–2,500 nm) and radiometric resolutions (16 bits) offer to match the rich spectral and spatial diversities; can potentially detect fine differences in spectral signatures; provide detailed fine spectral resolution data used to detect subtle differences in spectral reflectance; used for cover maps and measure leaf area index;	Less useful in highly turbid locations; limited to optically shallow waters (<20 m);
	Multispectral - high resolution (IKONOS, QuickBird, WorldView)	High spectral (2 band; 450–600 nm) and spatial (0.5–4 m) resolutions can reduce the number of mixed pixels; able to mapping at species composition level; match the rich spectral and spatial diversities;	Fewer water-penetrating bands costly compared to medium resolution for large spatial cover (>60 km) mapping; limited by water clarity;
	Multispectral - medium resolution (Landsat TM, ETM+, SPOT, ALOS, ASTER)	Spatial (10–30 m) and spectral resolutions (450–690 nm) are effective for repeatable mapping and monitoring across geographical scales; provides the large area coverage and longest continuous datasets; used for coarse descriptive level mapping in optically shallow water;	Poor spatial and spectral capabilities when useful signature can fall outside spectral ranges of visible bands; subtidal vegetation mapping is limited by water clarity; not possible for turbid water; cloud cover reduces number of images available;
	Multispectral - low resolution (MODIS, MERIS)	Low spatial resolution (250–500 m) with high spectral resolution (400–900 nm) enable to produce large spatial cover map and change analysis;	Unable to provide finer spatial details due to low spatial resolution; limited by water clarity and frequently result in systematic underestimation of the extent of seagrasses;
Aircraft	Laser (LiDAR)	Capable to measure bottom types at greater depth limit (1.5–60 m); can penetrate cloud cover;	Infrared region affected by water absorption (water column); tide levels introduce measurement errors; provide monochromic map with one variable (bottom reflectance);
	Hyperspectral (CASI, HyMap)	Offer information at many more spectral bands (~200 bands; 400–2,500 nm) located around typical absorption ranges provide more detailed distribution information of species and habitat;	Generally restricted to depths <6 m;
	Photographic film	Enable finer habitat discrimination;	Smaller area coverage than satellite;
Boat	Acoustic (single and multi-beam)	Used to map seagrass cover in areas with high seagrass biomass; mapping in deep water (>100 m); unconstrained by optical water properties;	Depends on seagrass species and biomass; limited use in shallow water (<0.5 m); clouds, strong winds, breaking waves; do not offer synoptic measurements over large areas;
Field	Visual (automatic underwater vehicle, diving, snorkeling, georeferenced photo and video)	Enable finer habitat discrimination; high data accuracy;	High time-cost and labor intensive; enable smaller area than remote sensing mapping.

tions across the remote sensing techniques and field-based survey for seagrass habitat mapping (Table 1).

The baseline knowledge on seagrass distribution derived from seabed habitat mapping is the key to understanding the present condition of seagrass communities in marine environments for sustainable management (Japar Sidik et al. 2006, Jagtap 1991, Muta Harah and Japar Sidik 2013). Moderate-resolution data such as Landsat (Yahya et al. 2010, Freeman et al. 2008, Hashim et al. 2001), SPOT (Barillé et al. 2010, Chen et al. 2013) and ALOS (Komatsu et al. 2009) have been routinely used to map seagrass resources in relatively shallow and clear waters. The Landsat is the only satellite that provides continuous global inventory data since 1972 (Wulder et al. 2008) on 16-day repeat cycle at no cost with 30 m pixel resolution, offers to map seagrass meadows from local (Yahya et al. 2010) to regional scale (Torres-Pulliza et al. 2013) and monitoring spatial and temporal changes (Lyons et al. 2012). Techniques developed for assessing changes in the seagrass environment are limited by existing approaches, because traditional image-based interpretations (pixel based classifications) of multispectral remote sensing data are typically sensor specific, site specific and often time specific (Kutser et al. 2006).

Issues related to water clarity (suspended materials, chlorophyll and colored dissolved organic matter) and depth limits are considered as major constraints for submerged aquatic vegetation mapping using optical remote sensing technologies (Wolter et al. 2005). To examine this inherent constrains of optical remote sensing, image enhancement techniques (ETs) are employed, as evident from recent researches. For example, integrated spatial and spectral enhancement techniques were demonstrated as an alternative method for mapping seagrass extent and density from high-resolution IKONOS imageries (Baumstark et al. 2012). Few studies documented applications of ETs on Landsat image to generate seagrass distribution map and monitor spatial and temporal changes (Knudby et al. 2010). Mapping of shallow and turbid seagrass habitats continues to be a challenge (Huang et al. 2014). Further research is required on the use of ETs and their ability to discriminate seagrass from other substrate under different coastal water settings (Baumstark et al. 2012). Hence, the aim of current study is to investigate the efficacy of using image ETs for detection boundary delineation and areal cover quantification of seagrass meadows in the subtidal and intertidal coastal areas of Sungai Pulai estuary, Johor Straits, Malaysia.

Data and methods

Study area

The open funnel shaped Sungai Pulai estuary, Johor Strait, Malaysia (1°13′–22′N, 103°31′–37′E) (Fig. 1) is situated on the south coast of Peninsular Malaysia was selected for this study. The estuary is relatively shallow (average depth 2.7 m) and water is highly turbid (Case II) (Annaletchumy et al. 2005). The tide is diurnal (2 low and 2 high tides in a 24 hours) and asymmetrical, ranging from −0.36 m during lowest spring tide to 3.2 m during spring tide. Seagrass meadows, namely Merambong shoal (henceforth termed as MS), Tanjung Adang Laut shoal (TALS) and Tanjung Adang Darat shoal (TADS) extend from the inland to the estuary of the Sungai Pulai river (Japar Sidik and Muta Harah 2003). They are characterized by soft sediment substrata, seagrass resources (seagrasses and macroalgae) and mangrove forests in the north (Japar Sidik et al. 2006). *Enha-*

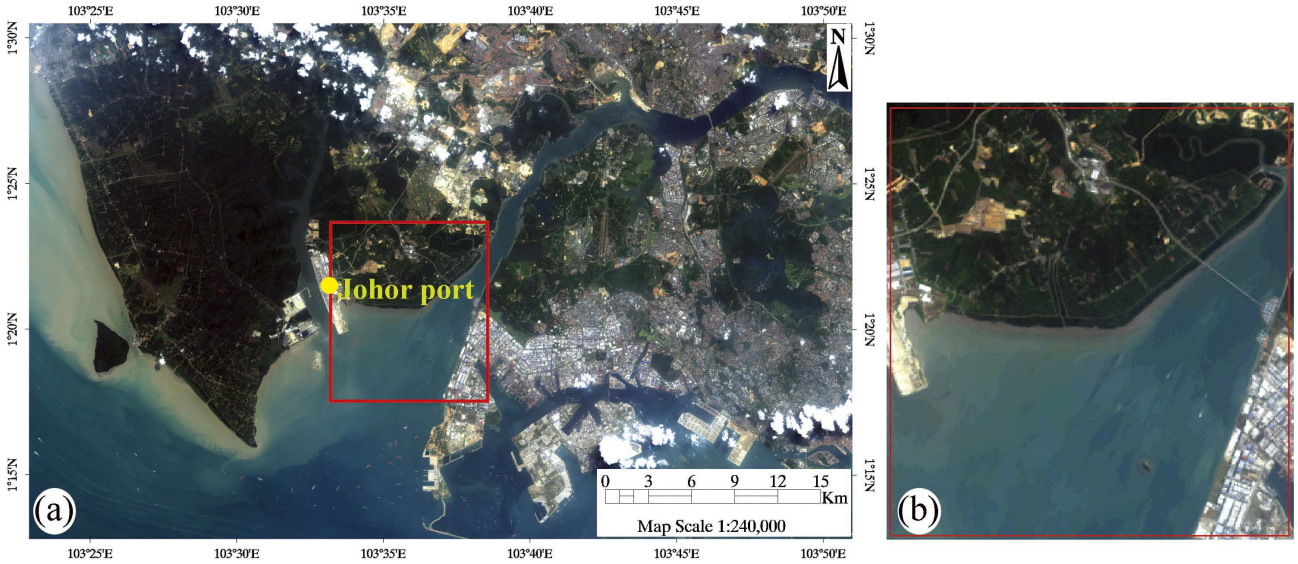

Fig. 1. Location of study site; image subset (panel a) showing Merambong shoal, Johor port and surrounding areas; focused region (panel b) used for analysis; red color box indicates location of the focused region for TM8 acquired on June 27, 2013.

lus acoroides and *Halophila ovalis* complex dominate the seagrass meadow (Cob et al. 2009).

Satellite data and analysis

Images of three Landsat satellite sensors—Landsat 5 (TM5), Landsat 7 (ETM+) and Landsat 8 (TM8) were used in this study. The single tile of WRS2 (Worldwide Reference System) path 125 row 59 cover the Sungai Pulai estuary and surrounding subtidal and intertidal areas. A total of 33 multi-date (1989–2014) images were downloaded from the web-server of Earthexplorer (http://earthexplorer.usgs.gov/). Scene attributes and values pertaining to this study were recorded from the metadata file (Table 2). All scenes were processed to L1T (Level 1 terrain corrected; geometrically corrected) by EROS data center. TM5 and ETM+ have three visible spectral bands (blue, green and red) for B1, B2 and B3, while TM8 have for B2, B3 and B4. These visible bands were used to generate true-color composites. Image subsets were cropped out from the whole scene to ease further analysis (Fig. 1 panel a). The Sungai Pulai estuary with surrounding subtidal and intertidal areas where seagrass meadows exist in higher concentration was marked as focused region (Fig. 1 panel b).

The Mean Sea Level Tide Height (MSLTH) predictive data were taken from the web interface facility at http://www.worldwidetide.com/. The interface holds the barotropic ocean tide height of every coordinate, following model developed by Egbert and Erofeeva (2002). The approximate center coordinate of Merambong shoal seagrass meadow (1°19′58.8″N, 103°35′59.6″E) was considered to be the reference point for predicting MSLTH during each scene acquisition time. The MSLTH ranges −0.281 to 0.234 m (Fig. 2). For the convenience of identification of respective images and presenting research results, all images were coded according to descending order of MSLTH (Table 2) in this paper.

Table 2. Sensor type, attribute and values of all Landsat images and input images employed for filling ETM+ SLC-off data-gaps in this study. Notes: UT=Universal Time; SC=Scene code.

Sensor	Acquisition date	Time (UT)	Sun elevation (degrees)	Sun azimuth (degrees)	SC	SLC-off gap-fill input
TM5	September 13, 1989	02:42	55.71	85.31	S22	
TM5	April 4, 1994	02:36	52.40	82.76	S17	
TM5	June 26, 1995	02:22	44.68	57.77	S29	
TM5	September 3, 1997	02:48	56.03	78.55	S23	
TM5	March 19, 2000	02:50	54.79	92.87	S33	
TM5	August 5, 2004	02:59	54.48	62.28	S6	
TM5	May 4, 2005	03:03	57.86	61.50	S20	
TM5	May 10, 2007	03:11	58.78	57.46	S15	
TM5	February 8, 2009	03:02	52.74	117.39	S31	
ETM+SLC-on	September 1, 1999	03:09	60.71	75.16	S2	
ETM+SLC-on	April 28, 2000	03:08	59.48	63.82	S18	
ETM+SLC-on	September 3, 2000	03:07	60.61	77.29	S9	
ETM+SLC-on	April 15, 2001	03:06	59.76	72.93	S5	
ETM+SLC-on	April 2, 2002	03:05	59.39	82.95	S4	
ETM+SLC-on	May 23, 2003	03:05	56.10	53.83	S13	
ETM+SLC-off	May 9, 2004	03:05	57.66	58.62	S1	S6
ETM+SLC-off	July 12, 2004	03:05	53.63	53.42	S19	S20
ETM+SLC-off	January 20, 2005	03:06	51.80	126.04	S24	S26
ETM+SLC-off	March 9, 2005	03:06	57.45	100.63	S32	S31
ETM+SLC-off	April 10, 2005	03:06	59.68	76.59	S26	S27
ETM+SLC-off	March 12, 2006	03:06	57.89	98.71	S27	S26
ETM+SLC-off	May 31, 2006	03:06	55.36	51.67	S3	S1
ETM+SLC-off	July 18, 2006	03:06	54.04	54.72	S16	S15
ETM+SLC-off	November 23, 2006	03:06	56.54	131.93	S25	S26
ETM+SLC-off	April 16, 2007	03:07	59.73	72.47	S30	S27
ETM+SLC-off	June 8, 2009	03:07	54.71	50.45	S28	S31
ETM+SLC-off	March 7, 2010	03:08	57.77	102.41	S7	S8
ETM+SLC-off	April 13, 2012	03:10	60.79	73.66	S8	S12
ETM+SLC-off	April 29, 2012	03:11	59.80	62.82	S12	S8
TM8	June 27, 2013	03:18	55.92	47.98	S10	
TM8	February 6, 2014	03:17	55.80	121.16	S11	
TM8	February 22, 2014	03:17	58.04	112.12	S14	
TM8	March 26, 2014	03:16	61.94	88.15	S21	

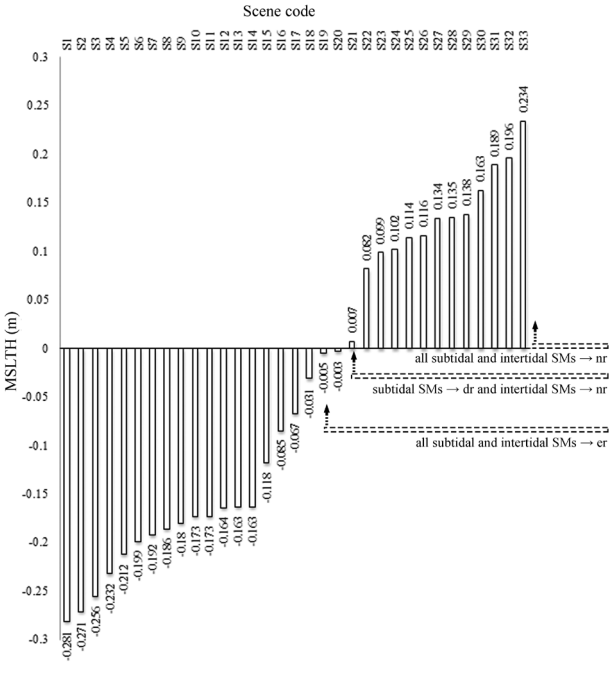

Fig. 2. Predicted MSLTH (m) data ranging from extreme lowest spring tide (S1=−0.281 m) to extreme highest spring tide (S33=0.234 m). MSLTH thresholds marked by dashed lines, illustrating ability to recognize seagrass meadows (SMs): er for 'easy-to-recognize', dr for 'difficult-to-recognize' or nr for 'not-recognizable'.

Image enhancement techniques

Two radiometric ETs—histogram equalization (HE) and manual enhancement (ME) were applied on the test images. Radiometric contrast enhancement basically transforms the histogram of the data, increasing contrast in some areas (considered as gain) and decreasing it in others and thus contrast can be lost between some Digital Numbers (*DNs*), while gained on others (Faust 1989). The histogram equalization is a non-linear stretch which transforms actual *DNs* to output Grey Level (*GL*s) space using Cumulative Distribution Function (*CDF*) (Eqn. 1) (Cihlar et al. 2001).

$$GL=255CDF\,(DN) \quad (1)$$

The ETs were applied on all actual images without any pre-processing (radiometric calibration, atmospheric or water-column corrections) except for the Weighted Linear Regression (WLR) algorithm integrated with Laplacian Prior Regularization Method (LPRM) (Zeng et al. 2013), were applied for filling data gaps in ETM+ SLC-off images. Closer image acquisition dates and similar MSLTH was considered while selecting image pairs for SLC-off data gap filling process because Gullström et al. (2006) has demonstrated that such image pairs do not require water column correction (Lyzenga 1978) due to small differences of water depth. Furthermore, there were no remarkable seagrass cover changes between the closer dates - a practical assumption, were considered prior to further image processing and seagrass coverage mapping in this study. The primary (ETM+ SLC-off image to be gap filled) and input (filler image of other date) images in the gap-filling process are listed in Table 2. The regularization parameter and maximum number of iteration were set to 0.01 and 600 respectively during implementation of LPRM method. The ETs techniques were applied using image enhancement tools of ENVI 5.0 (Exelis Visual Information Solutions, Inc., Boulder, USA). After several trials of adjusting brightness, contrast and transparency (sharpness in ENVI) of the satellite images, light to deep black seagrass meadows were clearly distinguishable from the non-seagrass habitats, i.e., deep to light blue water body in the subtidal areas and whitish (comparatively more brighter than intertidal seagrass cover) mudflat/sandy substrates in the intertidal areas. Similar methodological approach of color and textural contrasts were usually applied (e.g., Dolch et al. 2013) for visual interpretation of aerial color photograph with a view to identify seagrass meadows for intertidal mudflats. Thus, the perceived color contrast of the targeted objects allowed achieving the optimal level of true-color composite image brightness, contrast and sharpness controls as a result of ME in this study. The ME was applied manually by adjusting brightness, contrast and sharpness control tools from the respective 'default' values as 50, 20 and 10 of ENVI. Corresponding contrast levels for each scene are given in Table 3. The default function of ENVI (256 bins) was applied for automatic enhanced image generation by HE. The optimum contrast efforts achieved by employing the ETs, were not guided by the changes of multi-date MSLTHs and the GPS points that trace spatial extent of Merambong and Tanjung Adang Laut shoals. The later were used for map classification accuracy assessment (described in the section below).

ETs were applied only to improve the visual quality of the displayed image, the results of ETs cannot be compared by quantitative analysis (see page 206 of Schowengerdt and Schowengerdt 2007). Therefore, all the enhanced images were visually inspected and subjectively categorized based on image quality (IQ). Here, the 'image quality' referred to subjective level of targeted object distinctiveness to recognize/separate from surrounding non-targeted objects, image without loss of information, less noise and presence of sharp edge around the surrounding object, as described by Lillesand et al. (2008). IQ in regard to visual quality to recognize targeted objects (seagrass meadow, water body and mudflat areas) were thus, subjectively categorized as a) easy-to-recognize (er), b) difficult-to-recognize (dr) and c) not-recognizable (nr). The ET that delivered images with distinctive seagrass boundary at full extent, least noise and displayed clear borderline between water body and the seagrass meadows for subtidal areas and mudflat from intertidal seagrass meadows, were assessed as 'er' quality image. In

Table 3. The saturation contrast stretch values used for each actual image to achieve optimum enhanced image by ME technique.

	ME		
	Brightness	Contrast	Sharpness
S1	63	32	11
S2	84	59	17
S3	87	66	16
S4	66	42	20
S5	62	34	17
S6	67	40	15
S7	62	39	15
S8	80	40	22
S9	75	45	15
S10	56	26	16
S11	67	36	14
S12	89	64	20
S13	74	61	18
S14	69	49	25
S15	70	33	16
S16	68	27	15
S17	87	50	16
S18	85	64	18
S19	92	61	17
S20	69	44	16
S21	90	54	18
S22	69	39	18
S23	60	32	16
S24	64	32	15
S25	57	30	16
S26	56	27	13
S27	55	29	12
S28	60	27	12
S29	63	29	18
S30	76	34	14
S31	50	26	12
S32	60	30	11
S33	60	28	13

contrast, complete inability to display the distinctive characteristics of seagrass meadows were assessed as 'nr' image. The 'dr' IQ were marked when spatial extent of seagrass meadows were partly distinguishable; there is loss of seagrass spatial extent information compared to 'er' image and better visual quality than non-distinguishable targeted object of 'nr' image category.

Seagrass meadow boundary delineation and areal cover measurement

On-screen digitization approach has previously been used to classify seagrass from other substrates and boundary delineation. For example, meadow boundary was delineated by either color (RGB) or greyscale (black and white) color contrasts from aerial photography based on the color and texture of seagrass (e.g., Cuttriss et al. 2013), using true-color composites of Landsat imagery (B3, B2 and B1 layer stacks) based on visual interpretation made by local fishers (Lauer and Aswani 2008). Knudby et al. (2010) identified presence or absence of specific seagrass meadow from pixel brightness differences using the multi-temporal georeferenced images.

Separation of continuous features, i.e., sand, seagrass and water body was determined by visual assessment of cover; producing polygons around visually interpolated and extrapolated seagrass boundaries (Roelfsema et al. 2009) using the enhanced images and local knowledge. Manual digitization approach (see Roelfsema et al. 2013 and references therein), based on characteristics color contrasts was conducted for distinguishing the targeted objects. True color composites of enhanced images provided black with 48–62 of red (R), 51–52 of green (G) and 45–60 of blue (B) to dark brown with 92–112 of R, 75–92 of G and 90–105 of B for seagrass, that was distinguishable from dark blue with 55–66 of R, 78–90 of G and 91–102 of B to light blue with 117–119 of R, 191–193 of G and 190–240 of B surrounding water bodies in the subtidal areas and white with 208–231 of R, 189–195 of G and 178–180 of B to pink with 156–164 of R, 129–142 of G and 114–124 of B multitude of colors for sand in the subtidal areas. These color contrasts were used to separate objects, create polygons for specific seagrass cover and quantify areal cover. These visual assessments of seagrass cover map were implemented for twenty ME and HE preprocessed images acquired MSLTH −0.003 to −0.281 m (S1 to S20) and thus, clearly delineated MS, TALS and TADS seagrass meadow boundaries (Fig. 2) from non-seagrass substrates in this study.

Seagrass meadow delineation accuracy assessment

To locate the boundary of seagrass meadows a hand held GPS machine Colorado 300 was used. A total of 46 for MS and 37 for TALS GPS readings were taken on July 07, 2012 and March 31, 2013, respectively. During data collection, the MSLTH ranged from −0.231 m to −0.210 m on July 07, 2012 and −0.327 to −0.297 m on March 31, 2013. Ground truth GPS points were used as a source of reference data where polygon data were derived by joining those GPS data points for both MS and TALS. Another two polygons of MS and TALS seagrass meadows were generated by connecting GPS readings around the seagrass meadows from the produced enhanced images. Seagrass map accuracy was measured through comparing the input and the reference images. Thus, seagrass map accuracy was based on pixels intersecting the reference and input polygons. Five images acquired close to the GPS data collection dates, such as S8, S10, S11, S12 and S14 (Table 2) were used for developing confusion matrix and accuracy assessment. Map accuracy was estimated by means of overall accuracy along with Cohen's kappa, an alternative measure of accuracy between ref-

erence and resulting maps as informed by Cohen (1960) and Congalton (1991).

Results

Results of ETs to recognize subtidal and intertidal seagrass meadows

Results for HE and ME methods are presented in Table 4 and example data is illustrated in Fig. 3, to demonstrate the relations between visual recognition ability for subtidal and intertidal seagrass meadows with MSLTH changes from across the rows, while results among ETs are compared along the corresponding image in columns.

Image ETs substantially improved IQ compared to actual true-color composites as evident from the results obtained from optimally enhanced images irrespective of MSLTH regimes (panel a versus panel b or c in Fig. 3). Seagrass meadows were 'easy-to-recognize' (Fig. 2) from darker pixel visual impact than surrounding objects. For example, TADS (marked as d in Fig. 3) and 'Seluyong mudflat with seagrass meadow' (marked as b in Fig. 3) became recognizable as separate seagrass meadow when image contrast matches with MS and TALS. Multi-date images confirmed that information. HE in most cases over brightened particularly around the brighter object edges such as bare sand/mudflat areas and consequently failed to provide adequate Seluyong seagrass information (Table 4 and Fig. 3). Comparison

Table 4. Comparison of results of ET for ability to recognize intertidal and mudflat seagrass meadows. Notes: SC=Scene code; a=MS, b=seagrass with mudflat, c=TALS, d=TADS, er=easy-to-recognize, dr=difficult-to-recognize, nr=not-recognizable.

SC	MSLTH (m)	Outcome of the ET								Constrain
		HE				ME				
		a	b	c	d	a	b	c	d	
S33	0.234	nr	nr	nr	nr	nr	nr	nr	nr	Water column above MSL resulted inability to recognize seagrass meadows with ETs
S32	0.196	nr	nr	nr	nr	nr	nr	nr	nr	
S31	0.189	nr	nr	nr	nr	nr	nr	nr	nr	
S30	0.163	nr	nr	nr	nr	nr	nr	nr	nr	
S29	0.138	nr	nr	nr	nr	nr	nr	nr	nr	
S28	0.135	nr	nr	nr	nr	nr	nr	nr	nr	
S27	0.134	nr	nr	nr	nr	nr	nr	nr	nr	
S26	0.116	nr	nr	nr	nr	nr	nr	nr	nr	
S25	0.114	nr	nr	nr	nr	nr	nr	nr	nr	
S24	0.102	nr	nr	nr	nr	nr	nr	nr	nr	
S23	0.099	nr	nr	nr	nr	nr	nr	nr	nr	
S22	0.082	nr	nr	nr	nr	nr	nr	nr	nr	
S21	0.007	nr	nr	nr	nr	nr	nr	nr	nr	
S20	−0.003	dr	nr	nr	nr	dr	nr	nr	nr	
S19	−0.005	dr	dr	nr*	nr	dr	dr	nr*	nr	*Pixel noise constrained ability to recognize seagrass at c
S18	−0.031	er	dr*	er	er	er	dr*	er	er	*HE over-brightened image texture at b
S17	−0.067	er	dr*	nr	nr	er	dr*	nr	nr	*Cloud and cloud shadow cover hindered seagrass detection at b
S16	−0.085	er	dr*	er	nr	er	dr*	er	nr	*Cloud and cloud shadow cover hindered seagrass detection at b
S15	−0.118	er	er	er	nr	er	er	er	nr	
S14	−0.163	er	er	dr*	nr	er	dr*	er	nr	*Cloud and cloud shadow cover hindered seagrass detection at b
S13	−0.163	er	dr*	er	er	er	dr*	er	er	*Cloud and cloud shadow cover hindered seagrass detection at b
S12	−0.164	er	er	er	nr	er	er	er	nr	
S11	−0.173	er	er	er	nr	er	er	er	nr	
S10	−0.173	er	dr*	dr*	nr	er	er	er	nr	*HE over-brightened image texture at b and c
S9	−0.180	er	dr*	er	er	er	er	er	er	*HE over-brightened image texture at b
S8	−0.186	er	er	er	nr	er	er	er	nr	
S7	−0.192	dr*	er	er	nr	er	er	er	nr	*HE over-brightened image texture at b
S6	−0.199	er	er	dr*	nr	er	er	dr*	nr	*Cloud cover hindered seagrass detection at c
S5	−0.212	er	er	dr*	dr	er	er	dr*	dr	*Cloud and cloud shadow cover hindered seagrass detection at c
S4	−0.232	er	dr*	dr*	dr*	er	dr*	dr*	dr*	*Cloud and cloud shadow cover hindered seagrass detection at b, c, d
S3	−0.256	er	dr*	er	nr	er	dr*	er	nr	*Cloud cover partly obscured seagrass at b
S2	−0.271	er	dr*	er	er	er	dr*	er	er	*Cloud cover partly obscured seagrass at b
S1	−0.281	er	dr*	dr*	er	er	er	er	nr	*HE over-brightened image texture at b and c

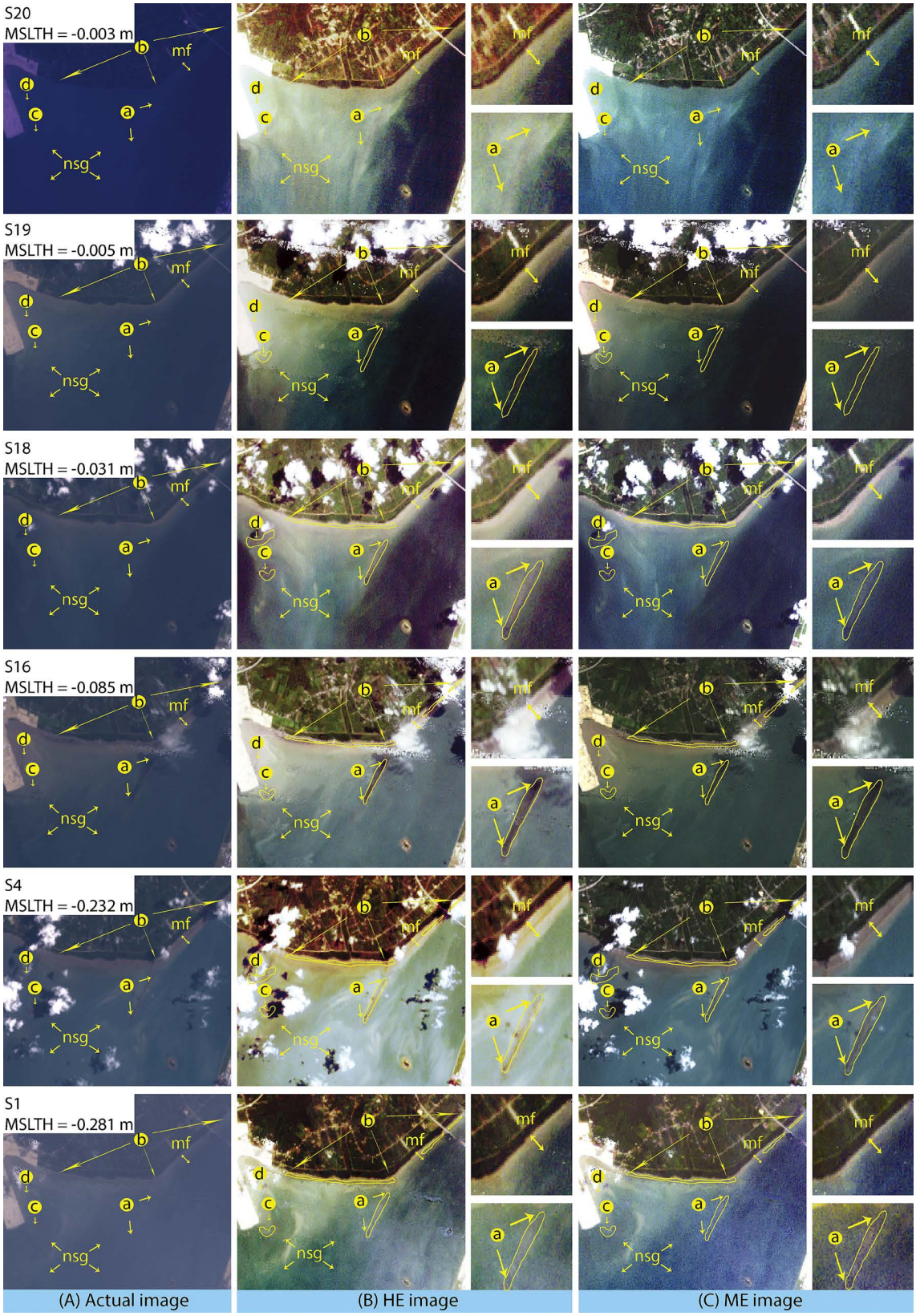

Fig. 3. Six actual (panel A) true-color composites example data of the focused region, illustrating ability of Landsat images to recognize spatial distribution of subtidal and intertidal seagrass meadows from results of HE (panel B) and ME (panel C) acquired in different dates at MSLTH regimes; seagrass meadows are marked by (a) at MS, (b) Seluyong mudflat with seagrass meadow, (c) TALS and (d) at TADS; mudflat extent as mf and non-seagrass/water body areas as nsg; zoomed-in view are taken from corresponding images illustrates results for intertidal mudflat with seagrass cover (top) and MS (bottom).

of multi-date images acquired at gradual decreased MSLTH demonstrated that they are closely related specially at higher MSLTH regimes. Seagrass meadows were 'easy-to-recognize' without noticeable variations due to MSLTH differences from the enhanced images acquired during extreme lowest spring tide height, −0.218 m and above until MSLTH at −0.085 m; also found 'difficult-to-recognize' at full extent between −0.067 to −0.003 m MSLTH and 'not-recognizable' (Fig. 2) above −0.003 m MSLTH. For example, there were no differences among image darkness due to presence of seagrass at MS as illustrated with zoomed-in view for S1 to S16 through S4 (bottom three rows of Fig. 3) while MSLTH difference was about 2 m between the maxima and minima. Results of HE and ME have proved ability to recognize all targeted objects from −0.281 m (S1) to −0.085 m (S16) MSLTH, while this MSLTH upper limit increased to −0.031 m and seagrass meadows were 'difficult-to-recognize' (Fig. 2) compared to former MSLTH for the enhanced images. MS was easy-to-recognize compared to TALS and mudflat from all images. Constant MS areal cover should also be noticeable from the multi-date enhanced images for all ETs, indicates no abrupt changes occurred in MS areal cover. TADS was recognizable from the images S4, 5, 9, 13 and 18 acquired from 1994 until 2003 while MSLTH ranges from −0.232 m to −0.031 m.

Visibility of mudflat was influenced by MSLTH regimes as evident from comparative analysis of both unenhanced and enhanced images. The width of mudflat was most clearly distinguishable from the edge of water body and mudflat at the lowest MSLTH (−0.281 m in this study), later gradually decreases with rising MSLTHs and at −0.005 m and above this substrate type was visible. The seagrass meadow at mf in Fig. 3 shows that Seluyong seagrass meadow areal cover detection was equivalently affected as of mudflat areas by MSLTH regimes but the degree of visibility varied with color contrast modified by ETs.

Seagrass areal cover and delineation accuracy assessment

Tables 5 presents total area of MS, TALS and TADS, Table 6 yearly cover change (%) and Table 7 presents results of mapping accuracy regard to ETs for MS and TALS. All the ETs produced visually similar quality images for MS, TALS and TADS which lead to clearly delineate their boundaries and precise measurement of areal cover (Fig. 4). Total area results per ET are nearly identical. There were negligible differences between areal cover measured from ME and HE pre-processed images (Table 5). The manually enhanced (ME) image of April 4, 1994 showed that TADS had the biggest areal cover with 40.3 ha than the MS (25.1 ha) followed by TALS (24.8 ha). TADS had experienced 30% (about 13 ha) seagrass spatial cover loss, while MS and TALS had

Table 5. Total seagrass meadow area (ha) results per ET. Data are presented in ascending order of scene acquisition date. Notes: SC=Scene code; SAD=Scene Acquisition Date; diff.=seagrass areal cover difference derived from polygon area between ME and HE results; - diff. when ME>HE; GT=groundtruthing; nr=not-recognizable because of non-existence of seagrass meadow; nr*=not-recognizable because of either cloud cover or higher MSLTH than threshold level.

SC	MSLTH (m)	SAD	MS			TALS			TADS			GT
			HE	ME	diff. (%)	HE	ME	diff. (%)	HE	ME	diff. (%)	
S17	−0.067	April 4, 1994	24.78	25.11	−1.3	23.48	24.75	−5.4	38.76	40.32	−4.0	No
S2	−0.271	September 1, 1999	25.77	26.53	−2.9	23.61	23.88	−1.1	37.11	37.64	−1.4	No
S18	−0.031	April 28, 2000	21.66	22.50	−3.7	23.04	23.55	−2.2	39.56	39.75	−0.5	No
S9	−0.18	September 3, 2000	23.62	23.68	0.3	23.87	23.24	2.6	12.26	12.96	−5.4	No
S5	−0.212	April 15, 2001	26.55	27.09	−2.0	15.03	15.84	−5.4	nr*	nr*		No
S4	−0.232	April 2, 2002	23.88	24.39	−2.1	14.89	13.61	8.6	12.32	12.94	−5.0	No
S13	−0.163	May 23, 2003	24.77	25.65	−3.6	10.57	11.19	−5.9	12.3	12.88	−4.7	No
S1	−0.281	May 9, 2004	28.35	29.43	−3.8	11.56	12.46	−7.8	nr	nr		No
S19	−0.005	July 12, 2004	22.38	23.44	−4.7	nr*	nr*		nr	nr		No
S6	−0.199	August 5, 2004	22.44	23.13	−3.1	11.82	11.69	1.1	nr	nr		No
S20	−0.003	May 4, 2005	16.74	17.82	−6.5	nr	nr		nr	nr		No
S3	−0.256	May 31, 2006	23.61	24.84	−5.2	11.89	11.33	4.7	nr	nr		No
S16	−0.085	July 18, 2006	29.89	29.06	2.8	11.02	11.54	−4.7	nr	nr		No
S15	−0.118	May 10, 2007	29.69	29.81	−0.4	10.36	10.63	−2.6	nr	nr		No
S7	−0.192	March 7, 2010	29.5	30.24	−2.5	11.42	11.83	−3.6	nr	nr		No
S8	−0.186	April 13, 2012	26.01	26.19	−0.7	11.64	11.79	−1.3	nr	nr		Yes
S12	−0.164	April 29, 2012	26.2	26.23	−0.1	11.06	12.22	−10.5	nr	nr		Yes
S10	−0.173	June 27, 2013	27.04	27.88	−3.1	11.22	11.61	−3.5	nr	nr		Yes
S11	−0.173	February 6, 2014	25.3	26.36	−4.2	11.62	12.32	−6.0	nr	nr		Yes
S14	−0.163	February 22, 2014	26.54	27.42	−3.3	11.4	11.52	−1.1	nr	nr		Yes

almost the same spatial extent with 23.7 ha and 23.2 ha respectively, as evident from the image of September 3, 2000. Although subsequent multi-date image analysis specifically images acquired on April 2, 2002 and May 23, 2003 showed existence of TADS but the complete loss of that seagrass meadow became evident from the image of May 9, 2004. In the years between 2006 and 2007 remained nearly stable with average areal cover of 27.9 ha for MS and 11.2 ha for TALS. No remarkable variations of MS and TALS seagrass spatial cover changes were evident from April 13, 2012 through June 27, 2013 until February 22, 2014 where, total areal cover measurements were ranging from 26.2–27.9 ha for MS and 11.5–12.3 ha for TALS (Table 5). An analysis of percent cover change per year presented in Table 6 for MS, TALS and TADS showed that in general, there were slow gain or loss of seagrass spatial cover when compared between 1994 and different years. The results showed that MS was found to be stable (estimated from % cover change year^{-1}); not temporally dynamic having both losses and gains within low ranges as between 1.70 to (–) 1.71 for gain and loss in May 09, 2004 and April 28, 2000 respectively. Similar stable cover change was also measured for TALS in between the years 1994 and all along different years acquired on May 23, 2003 until February 22, 2014, whilst, 5.1% loss year^{-1} occurred in April 15, 2001. Both the slow and dynamic trend of TADS seagrass loss year^{-1} was found until April 28, 2000 (0.2 to −1.2%) and September 03, 2000 (10.6%), respectively.

Table 6. Yearly percent cover change analysis between manually enhanced Landsat images acquired on April 4, 1994 from different years for MS, TALS and TADS; a positive figure indicates seagrass cover gain between images; nm*=spatial extent is non-measurable because of either cloud cover or higher MSLTH than threshold level.

Year	Areal cover change per year (%)		
	MS	TALS	TADS
April 4, 1994–September 1, 1999	1.04	–0.65	–1.23
April 4, 1994–April 28, 2000	–1.71	–0.80	–0.23
April 4, 1994–September 3, 2000	–0.89	–0.95	–10.57
April 4, 1994–April 15, 2001	1.12	–5.12	nm*
April 4, 1994–April 2, 2002	–0.36	–5.63	–8.49
April 4, 1994–May 23, 2003	0.24	–5.99	–7.45
April 4, 1994–May 9, 2004	1.70	–4.91	
April 4, 1994–July 12, 2004	–0.65	nm*	
April 4, 1994–August 5, 2004	–0.76	–5.10	
April 4, 1994–May 31, 2006	–0.09	–4.46	
April 4, 1994–July 18, 2006	1.28	–4.34	
April 4, 1994–May 10, 2007	1.43	–4.35	
April 4, 1994–April 13, 2012	0.24	–2.90	
April 4, 1994–April 29, 2012	0.25	–2.80	
April 4, 1994–June 27, 2013	0.57	–2.76	
April 4, 1994–February 6, 2014	0.25	–2.53	
April 4, 1994–February 22, 2014	0.46	–2.69	

The total areal cover for MS and TALS meadows were further re-validated by mapping accuracy assessment measures. The OA ranges between 87.54 to 99.99% for ME while 87.52–99.99% for HE (Table 7). All OAs were above 85%, indicating good delineation scheme.

Discussion

Seagrass recognition from enhanced image

The results indicated that there were significant improvements in IQ compared to actual image (without enhancement). Illustrations (Fig. 3) have demonstrated the ability of Landsat to distinctively recognize seagrass from surrounding substrate types. Similarly, simple display of true-color composites and classified images of TM5 and ETM+ were used successfully for monitoring spatial extent of coral, algae and seagrass dominating Chumbe islands in

Table 7. Seagrass meadow delineation accuracy per ET. Data are presented in ascending order of scene acquisition date.

SC	MSLTH (m)	Scene acquisition date	HE		ME	
			OA (%)	Kappa	OA (%)	Kappa
S8	–0.186	April 13, 2012	99.99	0.8119	99.99	0.8812
S12	–0.164	April 29, 2012	99.99	0.7855	99.99	0.7107
S10	–0.173	June 27, 2013	87.52	0.7411	87.54	0.7962
S11	–0.173	February 6, 2014	88.07	0.7105	89.91	0.7537
S14	–0.163	February 22, 2014	89.66	0.7763	89.10	0.9554

Zanzibar, and also proved to be effective tool over the supervised classification method (Knudby et al. 2010). The authors did not assess the tide height (MSLTH) that determines magnitude of detection in their methodology and thus, results could not be compared with this study. Potential use of ETs on Landsat images to discriminate seagrass from other substrate types and monitor seagrass cover changes are witnessed from other researches (Gullström et al. 2006, Knudby et al. 2010, Palandro et al. 2003, Torres-Pulliza et al. 2013, Wabnitz et al. 2008). The present study illustrated the enhanced image can detect seagrass meadow including Seluyong mudflat, which was not previously documented (Muta Harah and Japar Sidik 2013). The seagrass/algae distribution maps on the sand/mud flat area for the Straits of Malacca was conducted using SPOT and Landsat data acquired at low tide where images were analyzed with hierarchical unsupervised classification, followed by contextual editing for discriminating seagrass from surrounding substrates (sand/mudflat) and other vegetation (algae) (Ping Chen et al. 2013). The authors also noted that two usual causes such as water turbidity and depth made the classification scheme difficult and to achieve mapping accuracy at adequate level. To avoid water depth and clarity problems optimal set of Landsat images acquired at low tide heights were used for ecoregional scale seagrass mapping in the Lesser Sunda ecoregion (Torres-Pulliza et al. 2013). Thus, previous studies also indicated the capability of Landsat imageries that, when acquired at low tide heights were less challenging for seagrass distribution mapping from local to large spatial scale, compared to images acquired at high tide heights.

Seagrass recognition ability and MSLTH relations

Although image ET substantially improved image quality so as to visually recognize seagrass meadows, in most cases, HE over brightened the images in the mudflat area and eventually reduced clear visibility for Seluyong seagrass cover information extraction, as evident from the present study results (Fig. 3). Similarly, Kaliraj and Chandrasekar (2012) failed to discriminate between sand dunes and beaches because HE homogeneously brightened the objects. The results HE while assessed in terms of total areal cover of seagrass meadows indicated the ability to detect small sized seagrass patches like TALS (11.52–12.32 ha for ME; Table 5) within the MSLTH threshold limit (above −0.085 m) with negligible difference than ME. The present study found MSLTH threshold as −0.085 m at which all ETs produced quality image; gradually degrade image visual quality from 'easy-to-recognize (er)' to 'difficult-to-recognize (dr)' until −0.003 m (Fig. 2). All ETs showed inability to recognize subtidal and intertidal seagrass meadows at the higher levels of MSLTH (Fig. 3 and Table 4). It can commonly be stated that image enhancement techniques can be an efficient tool for the seagrass meadows those emerge to the sea surface during the low MSLTH. However, a particular range (threshold) of MSLTH could not be proposed for achieving an optimally enhanced image because MSLTH may fluctuate with topography of the seagrass beds. In this study, we limited influence of water quality and depth effect by considering optically shallow (turbid) water areas of 2.7 m average MSL depth. Therefore, our MSLTH thresholds are valid for only intertidal and shallow subtidal areas similar to Sungai Pulai estuary, where water depth ranges between 2.0–3.4 m (retrieved from http://www.worldwidetide.com) and Secchi disk depth is 0.5–1.0 m. Interpretations of seagrass detection and subsequent analysis of cover changes in areas deeper than our case study site will limit the detection of seagrass meadow changes. Nevertheless, the results of ETs support the commonly held assumptions: a) if the sea depth is higher, combined with steep slope (topographic feature) than Sungai Pulai estuary, the threshold will change to small value and b) if the water clarity is optically deep, i.e., underwater visibility is clearer than Sungai Pulai estuary, the threshold will change to high value. Therefore, considering the on-the-ground scenarios, especially with respect to water depth and clarity being inherent complex environmental characteristics of the seagrass occurring areas outside the Sungai Pulai estuary, is obvious and simultaneously MSLTH threshold will change. The greater advantage of improving image quality through ETs still persist and will add value to the existing image processing method and knowledge for seagrass applications.

Results also indicate that a particular range (threshold) of brightness, contrast and sharpness values (Table 3) and could not be proposed for achieving an optimally enhanced image because actual source IQ may fluctuate with sensors type (TM5 often provide poor quality images than ETM+ or TM8), solar illumination during image acquisition time and other local environmental settings. Image ETs still have promising results and this study provides practical information through qualitative and quantitative analysis that will provide useful input for further research.

The present study was performed without any correction applied to the multi-date images, acquired at a range of MSLTHs. However, ETs would be ineffective if applied to images acquired higher than MSL. Variations in water depth and clarity due to MSLTHs and study locations are also expected and will require water depth corrections. Water quality corrections are difficult to conduct accurately in the coastal water settings (Hu et al. 2001). It may be possible to apply instead ETs to improve visual quality of different images and extract seagrass information, acquired at closer MSLTHs.

In summary, this study suggests ME approach as more appropriate ET for seagrass applications based on following superior characteristics: a) retained all information which is

needed to recognize target from subjectively categorized quality image, able to visualize finer details of image content including presence of significant contrasts between targeted (seagrass, water body, mudflat) and unwanted (terrestrial) objects and detect seagrass meadows and quantitatively estimate the areal cover; b) equally treat 8-bits (TM5 and ETM+) and 16-bits (TM8) quantized data, help to generate equally distinctive targeted objects to discriminate valid number of classes for both intertidal and subtidal areas without loss of important seagrass areal cover information; d) potential to provide seagrass aerial cover change detection results similar in precision than more complex methods demanding absolute corrections (Andréfouët et al. 2001).

Benefits and constrains of ETs

The results of image ETs support the literature (Japar Sidik et al. 2006, Jagtap 1991, Muta Harah and Japar Sidik 2013) that described the consistent areal cover of MS and TALS, degradation of TADS after 2003 due to natural accumulation of thick gluttonous anoxic silt over that seagrass meadow. The multi-date image analysis witnessed the additional cause of sudden disappearance of TADS could be the land reclamation for extending facilities of Johor port (Fig. 1). The recent Landsat 8 image acquired at −0.191 m MSLTH during image acquisition time of July 16, 2014 shows the risk of MS seagrass habitat loss due to coastal land reclamation activity, began in early March, 2014 (Fig. 4 panel c). Sand deposits for land reclamation divided the MS into two segments—the landward northern (13.95 ha) and the seaward southern part (11.16 ha), reduced areal coverage from total 27 ha to 25.1 ha, i.e., a loss of 1.8 ha (~7%) seagrass bed, as estimated from optimally enhanced image. The complete loss of MS and including the nearby TALS is obvious once the proposed 49 ha land reclamation project will end. The detrimental impact for expansion of port (Port of Hastings) on seagrass habitats are evident in the recent impact assessment report, prepared for the Victorian National Parks Association Inc. (Kirkman 2013). There is considerable evidence that *Posidonia* meadows, and similar slow-growing seagrasses elsewhere in the world, can take decades to recover after a major disturbance (Kirkman 1997). This is not only consequence for *Posidonia* meadows but could also happen for seagrass meadows like TADS and MS. Once the TADS was disturbed may not naturally will be recovered even after 14 years as evident from change analysis of multi-date images 2003 to 2014, in this study. Furthermore, the static and consistent natural distribution of MS and TALS indicated that seagrass meadows were somewhat acclimated to the substrate they inhabit, any efforts to restore them with a view to regrow in somewhere else may not be successful (Japar Sidik and Muta Harah 2003).

The present study suggests a simple, straightforward and working-time saving approach of Landsat image analysis and

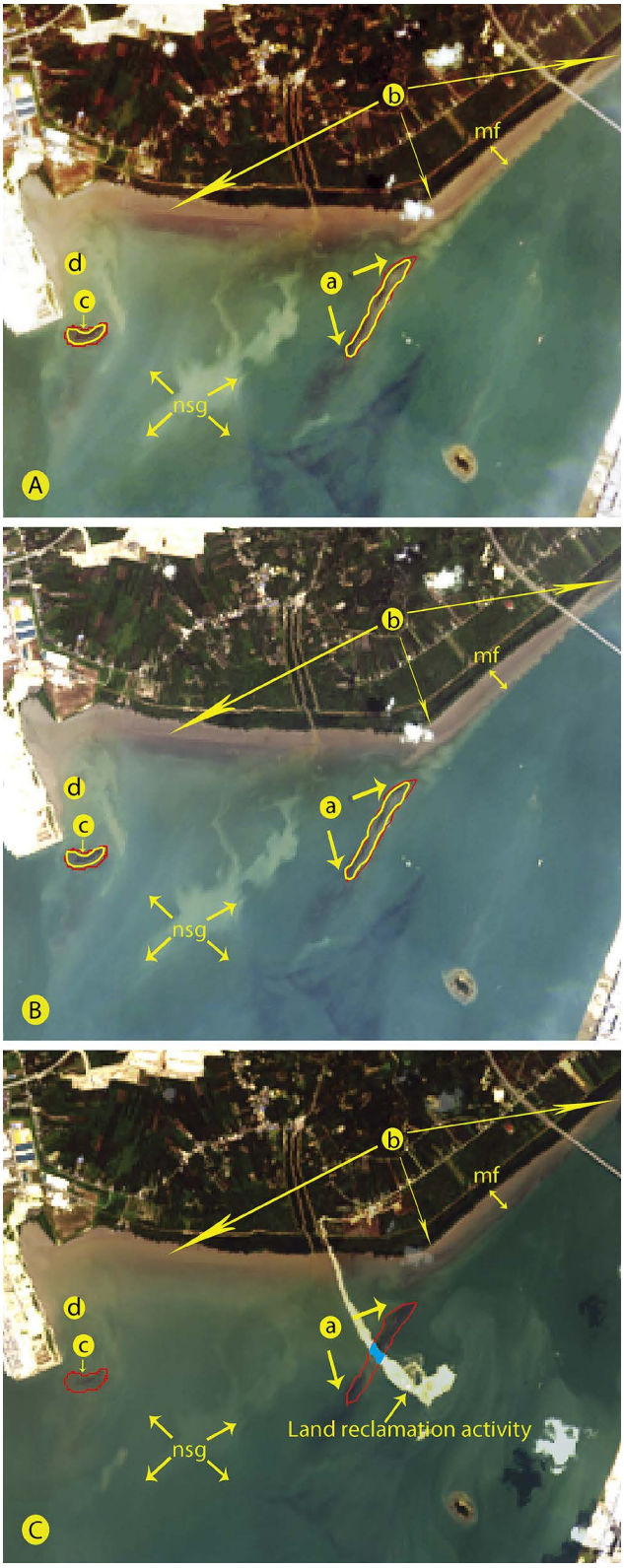

Fig. 4. Focused region of the study area from the TM8 image acquired on February 06, 2014 at −0.173 m MSLTH, illustrating results of HE (panel A) and ME (panel B) enhanced images and seagrass meadow detection technique for generating classified image; on-screen digitized and GPS-track data are marked by yellow and red polygons, respectively for MS (a) and TALS (c); location of Seluyong mudflat with seagrass is marked by b; TADS location is marked by d; loss of MS cover due to land reclamation activity is marked by cyan polygon in panel C from the manually enhanced (ME) TM8 image acquired on July 16, 2014.

interpretation technique that effectively improved the process of detection, boundary delineation and spatial extent quantification of seagrass meadows in turbid coastal waters of Sungai Pulai estuary, Malaysia. This paper outlined this alternative approach with comparable results among the ETs applied. The ME showed greater ability to recognize seagrass meadows than the HE. Selection of appropriate multi-date images based on MSLTH thresholds during image acquisition time for running image ETs, can be used to identify applicability of this alternative image processing routines (manual digitization of imagery) and generate seagrass distribution maps with acceptable accuracy (OA=87.54–99.99% for ME). The MSLTH data is obtainable from the website on per-pixel basis. The tools used for ETs is commonly available in free image processing software, such as QGIS (http://www.qgis.org), ImageJ (http://imagej.nih.gov/ij/), Bilko (http://www.ncl.ac.uk/tcmweb/bilko/index.shtml); indicate reproducibility of this approach for other case-specific studies.

These results of image ETs are however restricted by several uncontrolled factors. First: the quality of source image in terms of actual image brightness and contrast, for example, if blurred or noisy, will increase tasking difficulties for achieving quality image. Second: presence of cloud and cloud shadow cover over the targeted object (constrains reported in Table 4) is not repairable by applying ETs (Knudby et al. 2010). However, IQ issues are common when dealing with optical remote sensing.

Conclusion and future research

The manual ET from this study propose the alternative to operationally map seagrass habitats for subtidal and intertidal areas, provide local tide level during image acquisition time as critical environmental information for level of detection and map seagrass distribution from historical Landsat data sets; a critical input for monitoring and managing seagrass ecosystem health over space and time. The proposed approach extracts such information that includes a retrospective and baseline database of seagrass resources and presents the ability of multi-date Landsat images to provide us not only the estimate of seagrass areal cover change but also describe type of changes such as gain/loss, ecological process such as natural recovery (re-colonization) status after natural or human induced (land reclamation) disturbances and conservation issues (restoration). Other seagrass applications may be possible but must be considered on a case-by-case basis according to the seagrass bed topographic properties and environmental settings (water depth). Our future research plan is to test feasibility and transferability of the proposed ETs; re-validate it by applying to seagrass meadows of other locations with varying topography, water depth (MSLTH) and clarity conditions. Information derived from image ET can then be used for seagrass ecosystem health assessment, modeling and for better understanding of the ecological dynamics of seagrass communities.

Acknowledgements

This work was supported by the ScienceFund under Grant [project code: 04-01-04-SF1171] from the Ministry of Science, Technology and Innovation (MOSTI), Malaysia. This research was also a collaboration with the Asian Core program of Japan Society for the Promotion of Science (JSPS) and Establishment of research and education network on Coastal Marine Science in South East Asia. The authors would like to thank the Editor-in-Chief (Tomohiko Kawamura) and two anonymous reviewers, whose constructive comments and inputs significantly improved the paper.

Literature Cited

Andréfouët, S., Muller-Karger, F. E. E., Hochberg, J., Hu, C. and Carder, K. L. 2001. Change detection in shallow coral reef environments using Landsat 7 ETM+ data. Remote Sensing Environ. 78: 150–162.

Annaletchumy, L., Japar Sidik, B., Muta Harah, Z. and Arshad, A. 2005. Morphology of *Halophila ovalis* (R.Br.) Hook. f. from Peninsular and East Malaysia. Pertanika J. Trop. Agric. Sci. 28: 1–11.

Barillé, L., Robin, M., Harin, N., Bargain, A. and Launeau, P. 2010. Increase in seagrass distribution at Bourgneuf Bay (France) detected by spatial remote sensing. Aquat. Bot. 92: 185–194.

Baumstark, R., Dixon, B., Carlson, P., Palandro, D. and Kolasa, K. 2012. Alternative spatially enhanced integrative techniques for mapping seagrass in Florida's marine ecosystem. Int. J. Remote Sensing 34: 1248–1264.

Bouvet, G., Ferraris, J. and Andréfouët, S. 2003. Evaluation of large-scale unsupervised classification of New Caledonia reef ecosystems using Landsat 7 ETM+ imagery. Oceanol. Acta 26: 281–290.

Brown, C. J., S. Smith, J., Lawton, P. and Anderson, J. T. 2011. Benthic habitat mapping: A review of progress towards improved understanding of the spatial ecology of the seafloor using acoustic techniques. Estuarine, Coastal Shelf Sci. 92: 502–520.

Büttger, H., Nehls, G. and Stoddard, P. 2014. The history of intertidal blue mussel beds in the North Frisian Wadden Sea in the 20th century: Can we define reference conditions for conservation targets by analysing aerial photographs? J. Sea Res. 87: 91–102.

Chen, P., C., Liew, S. C., Lim, R. and Kwoh, L. K. 2013. Coastal and marine habitat mapping for the straits of Malacca using SPOT and Landsat data. Geoscience Remote Sensing Symp. (IGARSS): 2431–2434.

Cihlar, J., Okouneva, G., Beaubien, J. and Latifovic, R. 2001. A new histogram quantization algorithm for land cover mapping. Int. J. Remote Sensing 22: 2151–2169.

Cob, Z. C., Arshad, A., Japar Sidik, B. and Ghaffar, M. A. 2009. Species description and distribution of *Strombus* (Mollusca: Strombidae) in Johor Straits and its surrounding areas. Sains Malaysiana 38: 39–46.

Cohen, J. 1960. A Coefficient of Agreement for Nominal Scales.

Educ. Psychol. Meas. 20: 37–46.

Congalton, R. G. 1991. A review of assessing the accuracy of classifications of remotely sensed data. Remote Sensing Environ. 37: 35–46.

Cuttriss, A. K., Prince, J. B. and Castley, J. G. 2013. Seagrass communities in southern Moreton Bay, Australia: Coverage and fragmentation trends between 1987 and 2005. Aquat. Bot. 108: 41–47.

Dolch, T., Buschbaum, C. and Reise, K. 2013. Persisting intertidal seagrass beds in the northern Wadden Sea since the 1930s. J. Sea Res. 82: 134–141.

Egbert, G. D. and S. Erofeeva, Y. 2002. Efficient inverse modeling of barotropic ocean tides. J. Atmos. Oceanic Technol. 19: 183–204.

Faust, N. L. 1989. Image Enhancement. *In* Encyclopedia of Computer Science and Technology. Kent, A. and J. Williams, G. (eds.), pp. 1–416, Marcel Dekker, Inc., New York.

Ferwerda, J., Leeuw, J., Atzberger, C. and Vekerdy, Z. 2007. Satellite-based monitoring of tropical seagrass vegetation: current techniques and future developments. Hydrobiologia 591: 59–71.

Fortes, M. D. 2012. Historical review of seagrass research in the Philippines. Coastal Marine Sci. 35: 178–181.

Freeman, A. S., Short, F. T., Isnain, I. F., Razak, A. and Coles, R. G. 2008. Seagrass on the edge: Land-use practices threaten coastal seagrass communities in Sabah, Malaysia. Biol. Conserv. 141: 2993–3005.

GBO-3. 2010. Global Biodiversity Outlook 3. Available online at http://www.cbd.int/gbo3/ (accessed on April 28, 2014).

Gullström, M., Lundén, B., Bodin, M., Kangwe, J., Öhman, M. C., Mtolera, M. S. P. and Björk, M. 2006. Assessment of changes in the seagrass-dominated submerged vegetation of tropical Chwaka Bay (Zanzibar) using satellite remote sensing. Estuarine, Coastal Shelf Sci. 67: 399–408.

Hashim, M., Rahman, R. A., Muhammad, M. and Rasib, A.W. 2001. Spectral characteristics of seagrass with Landsat TM in Northern Sabah coastline, Malaysia. *In* 22nd Asian Conference on Remote Sensing, 5–9 November 2001, Singapore, pp. 128–132.

Hu, C., Muller-Karger, F. E., Andrefouet, S. and Carder, K. L. 2001. Atmospheric correction and cross-calibration of LANDSAT-7/ETM+ imagery over aquatic environments: A multiplatform approach using SeaWiFS/MODIS. Remote Sensing Environ. 78: 99–107.

Huang, C., Peng, Y., Lang, M., Yeo, I. and McCarty, G. 2014. Wetland inundation mapping and change monitoring using Landsat and airborne LiDAR data. Remote Sensing Environ. 141: 231–242.

Jagtap, T. G. 1991. Distribution of seagrasses along the Indian coast. Aquat. Bot. 40: 379–386.

Japar Sidik, B., Muta Harah, Z., Kanamoto, Z. and Mohd. Pauzi, A. 2001. Seagrass communities of the Straits of Malacca. *In* Aquatic resource and environmental studies of the Straits of Malacca: Current research and reviews. Japar Sidik, B., Arshad, A. Tan, S. G., Daud, S. K. Jambari, H. A. and Sugiyama, S. (eds.), pp. 81–98, Malacca Straits Research and Development Centre (MASDEC), Universiti Putra Malaysia, Serdang, Malaysia.

Japar Sidik, B. and Muta Harah, Z. 2011. Seagrasses in Malaysia. *In* Seagrasses: Resource Status and Trends in Indonesia, Japan, Malaysia, Thailand and Vietnam. Ogawa, H., Japar Sidik, B. and Muta Harah, Z. (eds.), pp. 22–37, Seizando-Shoten Publishing Co., Ltd., Tokyo.

Japar Sidik, B. and Muta Harah, Z. 2003. Seagrasses in Malaysia. *In* World Atlas of Seagrasses. Green, E. P. and Short, F. T. (eds.), Chapter 14, pp. 152–160, University of California Press, Berkeley, Los Angeles, London.

Japar Sidik, B., Muta Harah, Z. and Arshad, A. 2006. Distribution and significance of seagrass ecosystems in Malaysia. Aquat. Ecosyst. Health Manag. 9: 203–214.

Kaliraj, S. and Chandrasekar, N. 2012. Spectral recognition techniques and MLC of IRS P6 LISS III image for coastal landforms extraction along south west coast of Tamilnadu, India. Bonfring Int. J. Adv. Image Proc. 2: 1–7.

Kirkman, H. 2013. Impact of proposed Port of Hastings expansion on seagrass, mangroves and salt marsh. Report to Victorian National Parks Association, Melbourne Victoria.

Kirkman, H. 1997. Seagrasses of Australia. Australia: State of the Environment Technical Paper Series (Estuaries and the Sea), Department of the Environment, Canberra.

Knudby, A., Newman, C., Shaghude, Y. and Muhando, C. 2010. Simple and effective monitoring of historic changes in nearshore environments using the free archive of Landsat imagery. Int. J. Appl. Earth Observ. Geoinform. 12 Suppl. 1: 116–122.

Komatsu, T., Sagawa, T., Rhomdhane, H. B., Fukuda, M., Boisnier, E., Ishida, K., Belsher, T., Sakanishi, Y., Mohd, M. I. S., Ahmad, S. Lanuru, M., Mustapha, K. B. and Hattour, A. 2009. Utilization of ALOS AVNIR-2 data for mapping coastal habitats: Examples of seagrass beds from boreal to tropical waters. Proceedings of the ALOS PI Symposium, 3–7 November 2008, Island of Rhodes, Greece, SP-664, European Space Agency, January 2009.

Kutser, T., Vahtmäe, E. and Martin, G. 2006. Assessing suitability of multispectral satellites for mapping benthic macroalgal cover in turbid coastal waters by means of model simulations. Estuarine, Coastal Shelf Sci. 67: 521–529.

Lauer, M. and Aswani, S. 2008. Integrating indigenous ecological knowledge and multi-spectral image classification for marine habitat mapping in oceania. Ocean Coastal Manag. 51: 495–504.

Lillesand, T., Kiefer, R.W. and Chipman, J. 2008. Remote sensing and image interpretation. John Wiley and Sons, New York, USA.

Lyons, M. B., Phinn, S. R. and Roelfsema, C. M. 2012. Long term land cover and seagrass mapping using Landsat and object-based image analysis from 1972 to 2010 in the coastal environment of South East Queensland, Australia. ISPRS J. Photogram. Remote Sensing 71: 34–46.

Lyzenga, D. R. 1978. Passive remote sensing techniques for mapping water depth and bottom features. Appl. Optics 17: 379–383.

Malthus, T. J. and Mumby, P. J. 2003. Remote sensing of the coastal zone: An overview and priorities for future research. Int. J. Remote Sensing 24: 2805–2815.

Muta Harah, Z. and Japar Sidik, B. 2013. Occurrence and distribution of seagrasses in waters of Perhentian Island Archipelago,

Malaysia. J. Fish. Aquat. Sci. 8: 441–451.

Muta Harah, Z., Japar Sidik, B., Law, A. T. and Hishamuddin, O. 2000. Seedling of *Halophila beccarii* Aschers. in Peninsular Malaysia. Biologia Marina Mediterranea 7: 99–102.

Norhadi, I. 1993. Preliminary study of seagrass flora of Sabah, Malaysia. Pertanika J. Trop. Agric. Sci. 16: 111–118.

Palandro, D., Andréfouët, S., Muller-Karger, F. E., Dustan, P., Hu, C. and Hallock, P. 2003. Detection of changes in coral reef communities using Landsat-5 TM and Landsat-7 ETM+ data. Can. J. Remote Sensing 29: 201–209.

Petus, C., Collier, C., Devlin, M., Rasheed, M. and McKenna, S. 2014. Using MODIS data for understanding changes in seagrass meadow health: A case study in the Great Barrier Reef (Australia). Marine Environ. Res. 98: 68–85.

Roelfsema, C. M., Phinn, S. R., Udy, N. and Maxwell, P. 2009. An integrated field and remote sensing approach for mapping seagrass cover, Moreton bay, Australia. J. Spatial Sci. 54: 45–62.

Roelfsema, C., Kovacs, E. M., Saunders, M. I., Phinn, S., Lyons, M. and P. Maxwell. 2013. Challenges of remote sensing for quantifying changes in large complex seagrass environments. Estuarine, Coastal Shelf Sci 133: 161–171.

Schowengerdt, R. A. and Schowengerdt, R. A. 2007. Spectral transforms. *In* Remote sensing: models and methods for image processing. pp. 183–228, Elsevier, Amsterdam, Netherlands.

Torres-Pulliza, D., Wilson, J. R., Darmawan, A., Campbell, S. J. and Andréfouët, S. 2013. Ecoregional scale seagrass mapping: A tool to support resilient MPA network design in the Coral Triangle. Ocean Coastal Manag. 80: 55–64.

Wabnitz, C. C., Andréfouët, S., Torres-Pulliza, D., Müller-Karger, F. E. and Kramer, P. A. 2008. Regional-scale seagrass habitat mapping in the Wider Caribbean region using Landsat sensors: Applications to conservation and ecology. Remote Sensing Environ. 112: 3455–3467.

Wang, C. and Philpot, W. D. 2007. Using airborne bathymetric lidar to detect bottom type variation in shallow waters. Remote Sensing Environ. 106: 123–135.

Wolter, P. T., Johnston, C. A. and Niemi, G. J. 2005. Mapping submergent aquatic vegetation in the US Great Lakes using Quickbird satellite data. Int. J. Remote Sensing 26: 5255–5274.

Wulder, M. A., Ortlepp, S. M., White, J. C. and Maxwell, S. 2008. Evaluation of Landsat-7 SLC-off image products for forest change detection. Can. J. Remote Sensing 34: 93–99.

Xu, J. and Zhao, D. 2014. Review of coral reef ecosystem remote sensing. Acta Ecol. Sinica 34: 19–25.

Yahya, N. N., Mohd, M. I. S., Ahmad, S. and Komatsu, T. 2010. Seagrass and seaweed mapping using ALOS AVNIR-2 and Landsat-5 TM satellite data. Paper Presented at Malaysian Remote Sensing Society Conference, April 28–29 2010, Kuala Lumpur, Malaysia. Available on-line at: http://www.fksg.utm.my/remote_sensing/Remote%20Sensing%20Publications/2010/seegrass%20and%20seeweed%20mapping%20using%20alos%20avnir-2%20%28ibrahim%20seeni%29.pdf (accessed on June 5, 2014).

Zeng, C., Shen, H. and Zhang, L. 2013. Recovering missing pixels for Landsat ETM + SLC-off imagery using multi-temporal regression analysis and a regularization method. Remote Sensing Environ. 131: 182–194.